PHYSICAL REVIEW E **95**, 040401(R) (2017)

Effect of fractional blood flow on plasma skimming in the microvasculature

Jiho Yang,[1,2] Sung Sic Yoo,[1] and Tae-Rin Lee[1,*]

[1]*Advanced Institutes of Convergence Technology, Seoul National University, Suwon 443-270, Republic of Korea*

[2]*Department of Computer Science, Technische Universität München, Boltzmannstraße 3, Garching, Germany*

(Received 25 January 2017; published 25 April 2017)

Although redistribution of red blood cells at bifurcated vessels is highly dependent on flow rate, it is still challenging to quantitatively express the dependence of flow rate in plasma skimming due to nonlinear cellular interactions. We suggest a plasma skimming model that can involve the effect of fractional blood flow at each bifurcation point. To validate the model, it is compared with *in vivo* data at single bifurcation points, as well as microvascular network systems. In the simulation results, the exponential decay of the plasma skimming parameter M along fractional flow rate shows the best performance in both cases.

DOI: 10.1103/PhysRevE.95.040401

Red blood cells (RBCs) in microvessels are concentrated on the vessel core. Subsequently, a cell-free layer (CFL) with a thickness of a few micrometers is observed on the vessel wall. The CFL leads to an asymmetric redistribution of hematocrit at each bifurcation, called the plasma skimming effect. As a continuous process of plasma skimming in microvascular networks, the average hematocrit in capillary beds is lower than the systemic hematocrit as reported in many previous studies [1–8]. Interestingly, plasma skimming has recently been revisited to develop microchannels for detecting specific DNAs, proteins, and cells by efficiently separating plasma from whole blood [9–11]. Also, it has been highlighted to accurately predict drug carrier distribution in the microvasculature [12–18]. To utilize plasma skimming in applications *in vitro* and *in vivo*, it is crucial to quantitatively predict the redistribution of RBCs and plasma at bifurcations.

Since the early 1970s, several experiments for quantifying plasma skimming have been performed [2,19–23]. As pioneers, Pries *et al.* [24] measured plasma skimming regarding fractional blood flow in two different cases of the *in vivo* mouse model. The experiments confirmed previous studies that flow fractionation at the capillary entrance is an important determinant of capillary hematocrit, not the absolute flow velocity itself [2]. Then plasma skimming was expressed by the logit model considering fractional flow rate and vessel diameters [25]. This model matches well with previous experimental data at single bifurcations with specific curve fitting parameters. Recently, to improve the extensibility of the plasma skimming model to various conditions in microvascular networks, Gould and Linninger [26] suggested a model that can quantify plasma skimming with a single parameter M. Also, Lee *et al.* [16] introduced a generalized version of the plasma skimming model for cells and drug carriers.

In this paper we aim to mathematically model fractional blood flow in a simple and generalized manner in order to computationally study its significance in plasma skimming and also to accurately predict plasma skimming in the microvasculature. For this task, a recently developed plasma skimming model [26] is used and extended to take into account the effect of fractional blood flow. This model is then validated with experimental data at the single-bifurcation level and also at the microvascular network level.

While there are other plasma skimming models [25,27], the model developed by Gould and Linninger [26] is considered due to its easy extensibility. The model is as follows:

$$H_1 = H_0 - \Delta H = \zeta_1 H^*, \tag{1}$$

$$H_2 = \zeta_2 H^*, \tag{2}$$

$$Q_0 H_0 = Q_1 H_1 + Q_2 H_2 = Q_1 \zeta_1 H^* + Q_2 \zeta_2 H^*, \tag{3}$$

$$\zeta_i = \left(\frac{A_i}{A_0}\right)^{1/M} \quad \text{for } i = 1,2, \tag{4}$$

where H is the hematocrit, M is the plasma skimming parameter, ζ is the hematocrit change coefficient due to plasma skimming, Q is the flow rate, A is the cross-sectional area of each vessel, and the subscripts 0, 1, and 2 indicate the parent and two daughter vessels, respectively. Specifically, the plasma skimming parameter M is related to the cross-sectional distribution of RBCs near the bifurcation. Small M represents that RBCs are highly concentrated on the vessel core. In other words, the plasma dominant region, or CFL, is developed in the near-wall region. The two separated regions, expressed as RBCs and plasma areas, lead to strong plasma skimming. In contrast, high M means well-mixed RBCs and plasma. As a result, the plasma skimming effect will be diminished. Although plasma skimming is a function of hemodynamic parameters, M is fixed at a constant value $M = 5.25$ for the entire microvasculature [26] due to its complexity.

Here, to improve the plasma skimming model, the flow rate change from parent to daughter vessels is expressed by

$$M = M_0 e^{-k(Q_1/Q_0)}, \tag{5}$$

where M_0 and k are constant values for quantifying M as a function of fractional blood flow. In our simulation, M_0 and k are 10 and 4, respectively. Note that the subscript 1 denotes the daughter vessel with the largest diameter. Conceptually speaking, M can be considered as a ratio between the RBC collision force and hemodynamic lift force at the vessel wall. In this sense, if Q_1/Q_0 is low, the hemodynamic lift force at the corresponding daughter vessel is low compared to the RBC

*Corresponding author: taerinlee@snu.ac.kr

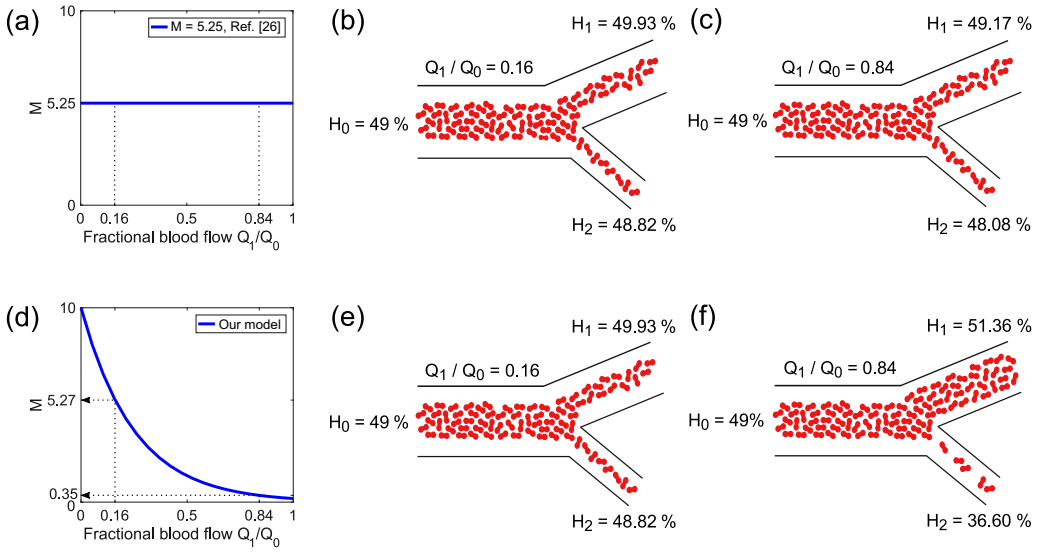

FIG. 1. Plots of plasma skimming parameter M against fractional blood flow and illustrations of RBC redistribution in two cases. Here Q_1/Q_0 denotes the fractional blood flow between the largest daughter vessel and parent vessel. (a)–(c) Without using the fractional blood flow model, there is negligible change in RBC redistributions at bifurcation since M is set as a constant. (d)–(f) When including the effect of fractional blood flow, both hemoconcentration and hemodilution after plasma skimming become more significant.

collision force and hence a high M value is obtained. This leads to a more uniform distribution of RBCs at the bifurcation. In contrast, high Q_1/Q_0 induces higher hemodynamic lift force, resulting in a low M value. Since, in this case, the RBCs are more likely to flow along the vessel core region towards the daughter vessel with a larger diameter, a stronger plasma skimming effect is produced. Therefore, the exponential decay function of M weakens the plasma skimming at low Q_1/Q_0 and vice versa. For instance, when Q_1/Q_0 is reduced, the natural flow tendency from the parent vessel to the daughter vessel with a larger diameter is disturbed and then well mixed at the bifurcation point. Under such circumstances, the hematocrit change from plasma skimming is small. On the other hand, at high Q_1/Q_0, the natural flow with a CFL from the parent vessel is prolonged to the daughter vessel with a larger diameter, leading to a hematocrit redistribution.

Figure 1 depicts plots of M against fractional blood flow and schematic illustrations of RBC redistribution with computed hematocrit values with and without the fractional blood flow model at a single bifurcation. For this computation, the hematocrit value at the parent vessel is set to 49% and the diameters of the parent and two daughter vessels are set to 20, 17.5, and 16.5 μm, respectively. Figure 1(a) shows the plot of M over fractional blood flow when M is set as a constant [26]. Figures 1(b) and 1(c) show the RBC redistributions when Q_1/Q_0 is 0.16 and 0.84, respectively. Since no relationship between the plasma skimming parameter and fractional blood flow was established in the original model, M remains as a constant. In this case, the change in RBC redistribution when varying Q_1/Q_0, for a given parent vessel hematocrit, is negligible.

Figure 1(d) presents the plot of M when Eq. (5) is applied. As shown in Fig. 1(e), the hematocrit change at $Q_1/Q_0 = 0.16$ is similar to that in Fig. 1(b) due to the similar M values. However, as described previously, incremental fractional blood flow produces greater plasma skimming and hence M is reduced. When Q_1/Q_0 is 0.84, M now becomes 0.35. As depicted in Fig. 1(f), rather significant change is observed in RBC redistribution compared with Fig. 1(c), where the difference in hematocrit between the daughter vessels becomes more significant. By considering the effect of fractional blood flow, both the hemoconcentration and hemodilution in the daughter vessels are amplified. Equation (5), with corresponding constants, as stated previously, is the only equation applied to model the effect of fractional blood flow.

In order to validate the fractional blood flow model, plasma skimming at the single bifurcation is computed and compared with *in vivo* experimental data [24], along with the model developed by Gould and Linninger [26]. The logit model [24,25] is not considered for a single bifurcation since this model was developed based on curve fitting of the same experimental data [24]. The physiological conditions as observed in the experiment are considered and this is summarized in Table I. Here H_0 denotes the hematocrit value at the parent vessel and d_0, d_1, and d_2 denote the diameters of the parent vessel and the two daughter vessels, respectively. The same fractional model of Eq. (5) is used for both geometries.

Figure 2 depicts the ratio of hematocrit H_i/H_0 for the two geometry cases from Table I. The fractional blood flow model matches very well with the experimental data, particularly in Fig. 2(b). While the model developed by Gould and Linninger [26] does not sufficiently capture the hemoconcentration and hemodilution, the fractional blood

TABLE I. Physiological conditions used for validation of the fractional blood flow model at a single bifurcation.

Case	H_0	d_0 (μm)	d_1 (μm)	d_2 (μm)
1	49%	20	17.5	16.5
2	43%	7.5	8	6

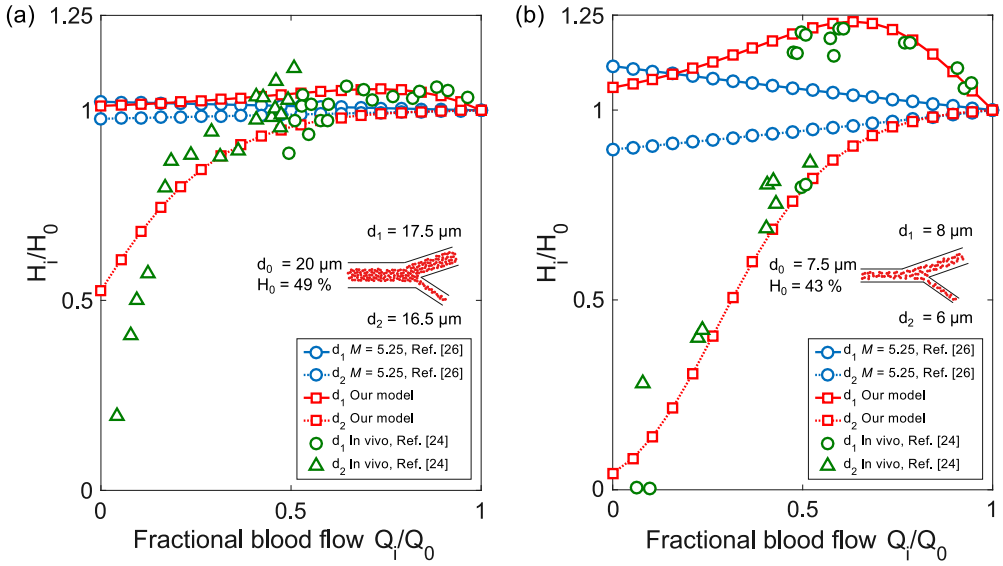

FIG. 2. Ratio of hematocrit between parent and daughter vessels (H_i/H_0) against fractional blood flow (Q_i/Q_0) at single bifurcation for comparing fractional blood flow model with the model developed by Gould and Linninger [26] and experimental data [24]. Two cases of geometries stated in Table I are considered. Significant amplifications in both hemoconcentration and hemodilution are produced by using fractional blood flow model, accurately matching the experimental data.

flow model significantly amplifies them. The value of H_1 from the fractional blood flow model in Fig. 2(b), for instance, increases up to 1.25, showing significant hemoconcentration. Similarly, H_2 from the fractional blood flow model shows very significant hemodilution down to 0.04 as Q_2/Q_0 decreases.

Figure 3 depicts H_i/H_0 for different k values. It must be noted that k is a highly sensitive parameter and must be chosen carefully, and as Fig. 3 shows, $k = 4$ gives the best match with the experimental data.

To predict the plasma skimming effect at the microvascular network level, the fractional blood flow model is coupled with a mathematical model of blood flow. A microvascular network model is computationally generated based on mathematical algorithms by choosing the vessel diameter d_i, vessel length l_i, and bifurcation angles θ_i and ϕ_i [16,28]. The diameters of the daughter vessels at each bifurcation are governed by $d_0^\gamma = d_1^\gamma + d_2^\gamma$, where γ is fixed at 3 [29,30]. The ratio of the two daughter vessels $\eta = d_2/d_1$ is utilized to control the geometric asymmetry of the entire microvascular network. With the diameter ratio η, the diameters of the daughter vessels are described by $d_1 = \sqrt[\gamma]{d_0^\gamma/[1 + N(\bar{\eta},\sigma^2)^\gamma]}$ and $d_2 = \sqrt[\gamma]{d_0^\gamma - d_1^\gamma}$, where N is a normal distribution with mean $\bar{\eta} = 0.62$ and standard deviation $\sigma = 0.1$ for capturing the heterogeneous diameter distribution.

The diameter of the root vessel is set to 40 μm and the cutoff diameter is set to 6 μm. Vessel lengths are governed by $l_i = \beta d_i^n$, where β is 100 and n is 0.46. As a boundary condition, the pressure difference between the root vessel and

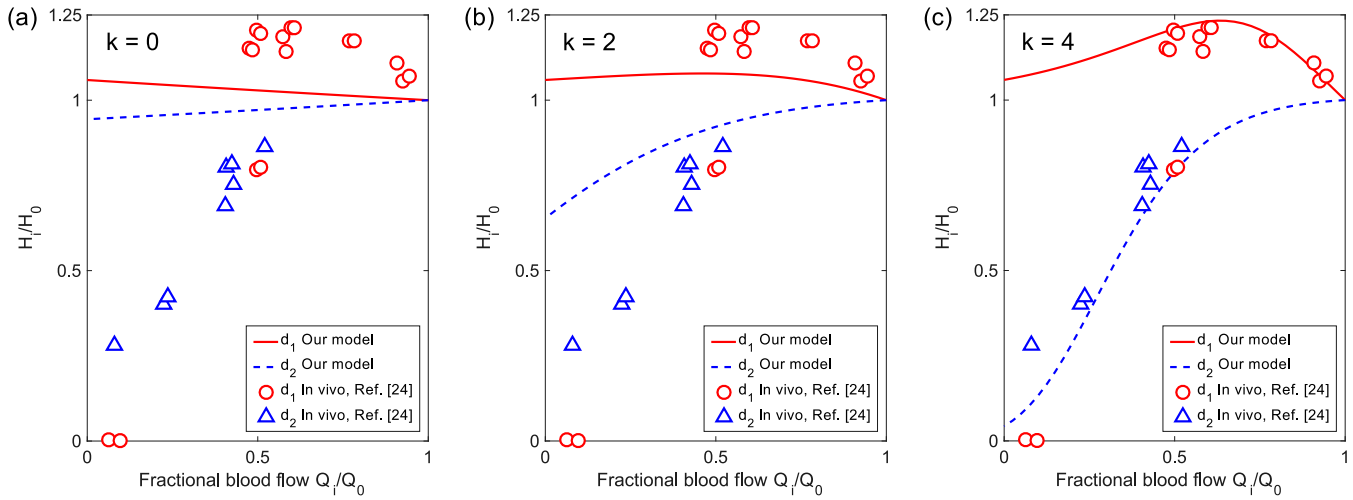

FIG. 3. Ratio of hematocrit between parent and daughter vessels (H_i/H_0) against fractional blood flow (Q_i/Q_0) at a single bifurcation for different k values. The second case stated in Table I is considered. The plots clearly show the high sensitivity of k and that $k = 4$ gives the best match with the experimental data [24].

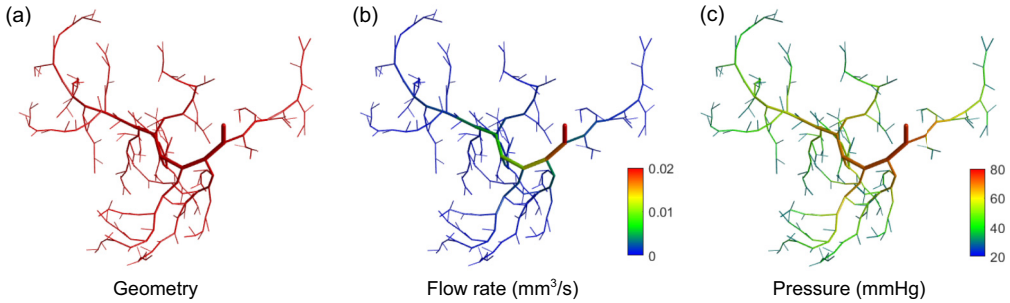

FIG. 4. Computational model of the microvascular network and the corresponding hemodynamic calculations.

the capillary ends is set to 47 mm Hg. The flow rate of blood flow Q_i is calculated by the Poiseuille flow model, using conservation of mass and *in vivo* viscosity laws [31] with the reference viscosity of plasma fixed at 9×10^{-6} mm Hg s [32]. To express the variation of systemic hematocrit, the initial hematocrit values have a range from 0.3 to 0.45. The plasma skimming is controlled by considering CFL thickness in the plasma skimming model as $M'/M = 1 + 10e^{-100\delta'}$, where δ' is the relative CFL with respect to vessel diameter, which is determined by a curve fitting of *in vivo* experiment data [33], $\delta' = (1.8e^{-6H}\sqrt{d - 5.0} + 0.5)/d$. The CFL function is applied in order to limit plasma skimming at highly RBC concentrated parent vessels. Since high hematocrit means a very thin CFL and hence no plasma skimming, if the CFL thickness is too small this function sets a high M to stop plasma skimming.

Figure 4 depicts the computationally generated microvasculature model and corresponding hemodynamic calculations. A systemic hematocrit of 45% is applied as an initial boundary condition. Figure 4(a) shows the microvasculature geometry used for predicting plasma skimming at the microvascular network level. Figures 4(b) and 4(c) show the computed flow velocity and pressure, respectively. Figure 5 shows the computed blood flow and hematocrit distribution along

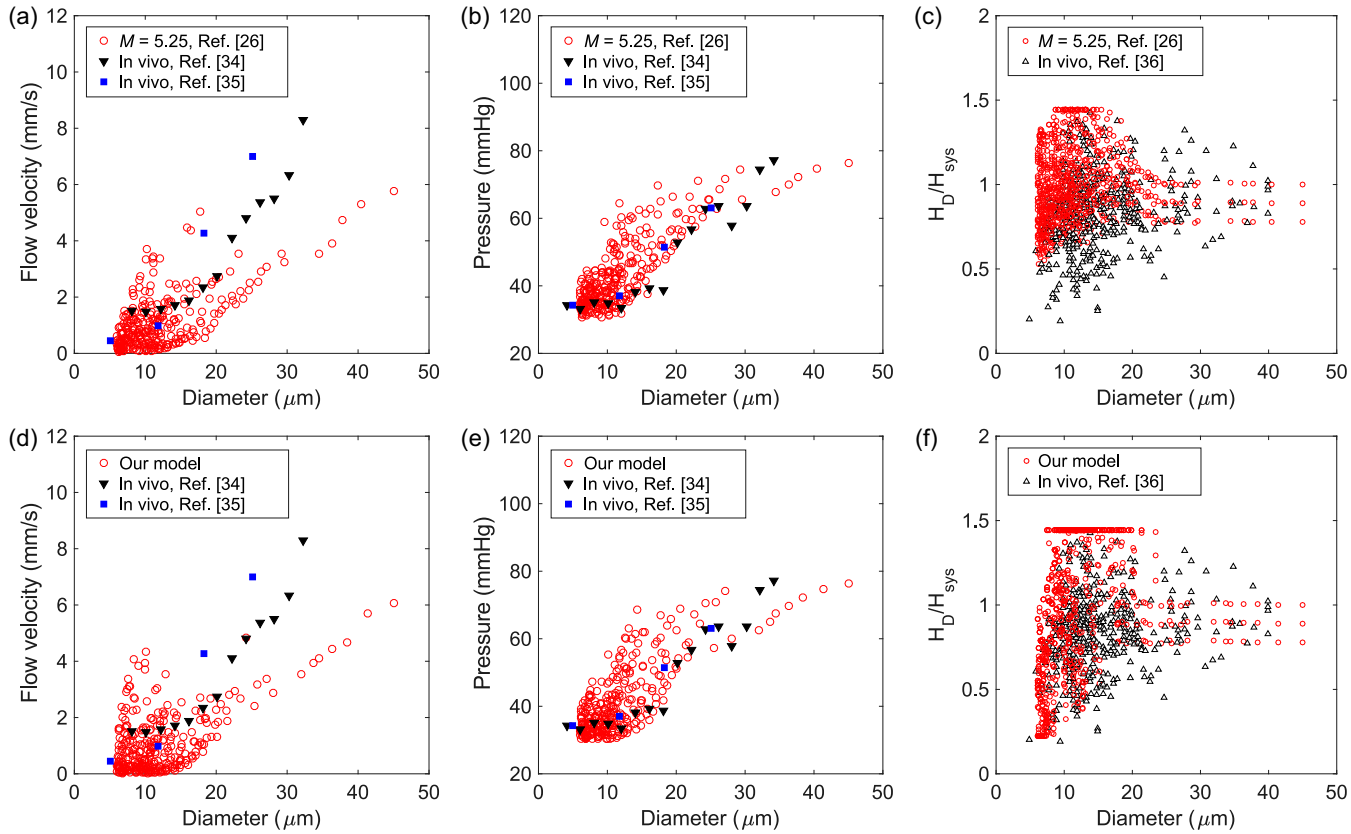

FIG. 5. Comparison of hemodynamic characteristics at the microvascular network level between (a)–(c) Gould and Linninger's model and (d)–(f) the fractional flow model. Vessel diameters are asymmetrically decreased from 40 to 6 μm. The pressure drop between the root vessel to capillary ends is set to 47 mm Hg. Flow velocity and pressure data are compared with two sets of *in vivo* experimental data [34,35]. Also shown is the relative hematocrit distribution along with vessel diameters for the microvascular network model. The systemic hematocrit H_{sys} is set to 0.45. Black triangles represent *in vivo* experimental data [36]. The initial hematocrit at the root vessel is varied from 0.3 to 0.45.

with vessel diameters. Two models, Gould and Linninger's model and the fractional blood flow model, are compared with *in vivo* flow velocity and pressure data [34,35] and *in vivo* hematocrit scatter data [36]. As plotted in the figures, the mathematical model considering the effect of fractional blood flow holds good agreement with *in vivo* data. From Fig. 5, one must note that application of the flow rate ratio effect does not significantly alter both flow velocity and pressure. This is because the most significant parameter for determining flow velocity is vessel diameter, as stated by Poiseuille's law. On the other hand, the flow rate ratio strongly influences hematocrit distribution since the most significant parameter for determining hematocrit is ζ, which is governed by M. Therefore, no significant change in flow velocity and pressure is visible despite a significant change in hematocrit distribution. Furthermore, numerous parameters at the network level correlate with the microvascular transport of blood. Hence, the sensitivity analysis of the plasma skimming model with flow rate dependence must be very carefully investigated at the microvascular network level. In this paper, we aim to solely study the effect of the fractional flow rate on plasma skimming. For this reason, same hematocrit cutoff conditions are applied to both models to compare the results under the same circumstances: an artificial cutoff value of relative hematocrit $H_D/H_{\mathrm{sys}} = 1.5$ and the modified M' by the CFL function. Both models capture the plasma skimming in capillary beds. However, unlike Gould and Linninger's model, which shows a dense hematocrit distribution in capillary beds particularly below 15 μm, the fractional blood flow model gives more sparsely dispersed hematocrit even below 10 μm. Such a distribution is obtained due to amplification in the plasma skimming effect induced by the fractional flow rate.

In conclusion, the effect of fractional blood flow on plasma skimming of RBCs in the microvasculature was mathematically designed and quantitatively predicted. As shown from the results, the fractional blood flow model accurately matches with *in vivo* experimental data, at both the single-bifurcation and microvascular network levels, indicating that fractional blood flow is an important parameter that must be taken into account in studying plasma skimming. Furthermore, these results quantitatively validate previous qualitative and experimental studies that fractional blood flow greatly affects plasma skimming.

This research was supported by the Basic Science Research Program of the National Research Foundation of Korea funded by the Ministry of Education (Grant No. 2015R1D1A1A01060992), and by the Bio and Medical Technology Development Program of the National Research Foundation of Korea funded by the Ministry of Science, ICT, and Future Planning (Grant No. 2016M3A9B4919711).

[1] J. Cohnstein and N. Zuntz, Pflügers Arch. Eur. J. Physiol. **42**, 303 (1888).
[2] P. C. Johnson, J. Blaschke, K. S. Burton, and J. Dial, Am. J. Physiol. **221**, 105 (1971).
[3] G. Schmid-Schoenbein and B. Zweifach, Microvasc. Res. **10**, 153 (1975).
[4] B. Klitzman and B. R. Duling, Am. J. Physiol. **237**, H481 (1979).
[5] H. H. Lipowsky, S. Usami, and S. Chien, Microvasc. Res. **19**, 297 (1980).
[6] G. Kanzow, A. R. Pries, and P. Gaehtgens, Bibliotheca. Anat. **20**, 149 (1981).
[7] G. Kanzow, A. Pries, and P. Gaehtgens, Int. J. Microcirc. **1**, 67 (1982).
[8] I. H. Sarelius, D. N. Damon, and B. R. Duling, Am. J. Physiol. **241**, H317 (1981).
[9] R. Fan, O. Vermesh, A. Srivastava, B. K. Yen, L. Qin, H. Ahmad, G. A. Kwong, C.-C. Liu, J. Gould, L. Hood *et al.*, Nat. Biotechnol. **26**, 1373 (2008).
[10] S. S. Shevkoplyas, T. Yoshida, L. L. Munn, and M. W. Bitensky, Anal. Chem. **77**, 933 (2005).
[11] M. Kersaudy-Kerhoas and E. Sollier, Lab Chip **13**, 3323 (2013).
[12] T.-R. Lee, M. Choi, A. M. Kopacz, S.-H. Yun, W. K. Liu, and P. Decuzzi, Sci. Rep. **3**, 2079 (2013).
[13] J. Tan, S. Shah, A. Thomas, H. D. Ou-Yang, and Y. Liu, Microfluid. Nanofluid. **14**, 77 (2013).
[14] K. Müller, D. A. Fedosov, and G. Gompper, Sci. Rep. **4**, 4871 (2014).
[15] T.-R. Lee, M. S. Greene, Z. Jiang, A. M. Kopacz, P. Decuzzi, W. Chen, and W. K. Liu, Biomech. Model. Mechanobiol. **13**, 515 (2014).
[16] T.-R. Lee, S. S. Yoo, and J. Yang, Biomech. Model. Mechanobiol. **16**, 497 (2017).
[17] J. Tan, W. Keller, S. Sohrabi, J. Yang, and Y. Liu, Nanomaterials **6**, 30 (2016).
[18] R. D'Apolito, F. Taraballi, S. Minardi, X. Liu, S. Caserta, A. Cevenini, E. Tasciotti, G. Tomaiuolo, and S. Guido, Med. Eng. Phys. **38**, 17 (2016).
[19] G. Schmid-Schönbein, R. Skalak, S. Usami, and S. Chien, Microvasc. Res. **19**, 18 (1980).
[20] H. Lipowsky, S. Rofe, L. Tannenbaum, J. Firrell, S. Usami, and S. Chien, Microvasc. Res. **21**, 249 (1981).
[21] B. Klitzman and P. C. Johnson, Am. J. Physiol. **242**, H211 (1982).
[22] G. Mchedlishvili and M. Varazashvili, Bull. Exp. Biol. Med. **93**, 550 (1982).
[23] B. M. Fenton, R. T. Carr, and G. R. Cokelet, Microvasc. Res. **29**, 103 (1985).
[24] A. Pries, K. Ley, M. Claassen, and P. Gaehtgens, Microvasc. Res. **38**, 81 (1989).
[25] A. R. Pries and T. W. Secomb, Am. J. Physiol. **289**, H2657 (2005).
[26] I. G. Gould and A. A. Linninger, Microcirculation **22**, 1 (2015).
[27] R. Guibert, C. Fonta, and F. Plouraboué, Transp. Porous Media **83**, 171 (2010).

[28] J. Yang, Y. E. Pak, and T.-R. Lee, Microvasc. Res. **108**, 22 (2016).
[29] C. D. Murray, J. Gen. Physiol. **9**, 835 (1926).
[30] T. F. Sherman, J. Gen. Physiol. **78**, 431 (1981).
[31] A. Pries, T. W. Secomb, and P. Gaehtgens, Cardiovasc. Res. **32**, 654 (1996).
[32] J. Yang and Y. Wang, Int. J. Numer. Methods Biomed. Eng. **29**, 515 (2013).
[33] N. Tateishi, Y. Suzuki, M. Soutani, and N. Maeda, J. Biomech. **27**, 1119 (1994).
[34] A. Pries, T. W. Secomb, and P. Gaehtgens, Am. J. Physiol. **269**, H1713 (1995).
[35] L. Gagnon, S. Sakadžić, F. Lesage, E. T. Mandeville, Q. Fang, M. A. Yaseen, and D. A. Boas, Neurophotonics **2**, 015008 (2015).
[36] A. Pries, K. Ley, and P. Gaehtgens, Am. J. Physiol. **251**, H1324 (1986).